

$X(3872) \rightarrow J/\psi \pi^+ \pi^-$ AND $X(3872) \rightarrow J/\psi \pi^+ \pi^- \pi^0$ DECAY WIDTHS FROM QCD SUM RULES

F.S. Navarra and M. Nielsen

Instituto de Física, Universidade de São Paulo, C.P. 66318, 05389-970 São Paulo, SP, Brazil

New spectroscopy from the B factories, the advent of CLEO-c and the BES upgrade renewed the interest in charmonia. Among the new measurements, the state $X(3872)$ has received special attention due to its unexpected properties. Its structure has been studied with different theoretical approaches, most of them being able to reproduce the measured mass. A further test for the theoretical descriptions of the $X(3872)$ is to explain its narrow decay width. In this work we address the decays $X \rightarrow J/\psi \pi^+ \pi^- \pi^0$ and $X \rightarrow J/\psi \pi^+ \pi^-$, using QCD sum rules with the hypothesis that X is a four quark state.

PACS numbers: 11.55.Hx, 12.38.Lg, 12.39.-x

During the last three years several new hadronic states have been observed, as for example the $D_{sJ}^+(2317)$ [1] and the $X(3872)$ [2]. The experimental observations were always followed by theoretical efforts to understand the basic properties of the new particles, in particular the mass and the decay width. In the charm sector, simple potential models, which had been so successful in the past, failed in reproducing the masses of the new states. This was taken as an indication that these particles are not simple $q - \bar{q}$ bound states. As for the very narrow decay width, whereas it is expected in the case of the $D_{sJ}^+(2317)$, since it decays through an isospin violating channel, in the case of the $X(3872)$ it is really surprising. Even more surprising is the observation, reported by the BELLE collaboration [3], that the X decays to $J/\psi \pi^+ \pi^- \pi^0$, with a strength that is compatible to that of the $J/\psi \pi^+ \pi^-$ mode:

$$\frac{Br(X \rightarrow J/\psi \pi^+ \pi^- \pi^0)}{Br(X \rightarrow J/\psi \pi^+ \pi^-)} = 1.0 \pm 0.4 \pm 0.3. \quad (1)$$

This decay suggests an appreciable transition rate to $J/\psi \omega$ and establishes strong isospin violating effects. The measured $X(3872)$ mass can be reproduced in several approaches and it is not yet possible to discriminate between the different structures proposed for this state: tetraquark [4, 5], cusp [6], hybrid [7], glueball [8] or $D\bar{D}^*$ bound state [9, 10, 11, 12, 13].

The theoretical study of the decay width can help in clarifying this situation. In this work we use the method of QCD sum rules (QCDSR) [14, 15, 16] to study the hadronic decays of $X(3872)$ given in Eq.(1), considering X as a four-quark state. In recent calculations [17, 18, 19], the QCDSR approach was used to study the light scalar mesons, the $D_{sJ}^+(2317)$ meson and the $X(3872)$ meson considered as four-quark states and a good agreement with the experimental masses was obtained. In particular, in ref.[19] we have considered the $X(3872)$ as the $J^{PC} = 1^{++}$ state with the symmetric spin distribution: $[cq]_{S=1}[\bar{c}\bar{q}]_{S=0} + [cq]_{S=0}[\bar{c}\bar{q}]_{S=1}$. The interpolating field for X_q is given by:

$$j_\mu^q = \frac{i\epsilon_{abc}\epsilon_{dec}}{\sqrt{2}}[(q_a^T C \gamma_5 c_b)(\bar{q}_d \gamma_\mu C \bar{c}_e^T) + (q_a^T C \gamma_\mu c_b)(\bar{q}_d \gamma_5 C \bar{c}_e^T)], \quad (2)$$

where a, b, c, \dots are colour indices, C is the charge conjugation matrix and q represents the quark u or d .

As pointed out in [4], isospin forbidden decays are possible if X is not a pure isospin state. Pure isospin states are:

$$X(I=0) = \frac{X_u + X_d}{\sqrt{2}}, \quad \text{and} \quad X(I=1) = \frac{X_u - X_d}{\sqrt{2}}. \quad (3)$$

If the physical states are just X_u or X_d , the mass eigenstates, maximal isospin violations are possible. Deviations from these two ideal situations are described by a mixing angle between X_u and X_d [4]:

$$\begin{aligned} X_l &= X_u \cos \theta + X_d \sin \theta, \\ X_h &= -X_u \sin \theta + X_d \cos \theta. \end{aligned} \quad (4)$$

In ref. [4], by considering the ratio of branching ratios given in Eq.(1), they arrived at $\theta \sim 20^\circ$ and at $\Gamma(X \rightarrow J/\psi \pi \pi) \sim 5$ MeV. However, to arrive at such small decay width they had to make a bold guess about the order of magnitude of the $XJ/\psi V$ (where V stands for the ρ or ω vector meson) coupling constant: $g_{X\psi V} = 0.475$. In this work we evaluate the $XJ/\psi V$ coupling constant directly from the QCD sum rules. For the light scalar mesons, considered as diquark-antidiquark states, the study of their vertex functions using the QCDSR approach was done in ref.[17]. The hadronic couplings determined in ref.[17] are consistent with existing experimental data. In the case

of the meson $D_{sJ}^+(2317)$ considered as a four-quark state, the QCDSR evaluation of the hadronic coupling constant $g_{D_{sJ}D_{s\pi}}$ [20] gives a partial decay width in the range $0.2 \text{ keV} \leq \Gamma(D_{sJ}^+(2317) \rightarrow D_s^+\pi^0) \leq 40 \text{ keV}$.

The QCDSR calculation for the vertex, $X(3872)J/\psi V$, centers around the three-point function given by

$$\Pi_{\mu\nu\alpha}(p, p', q) = \int d^4x d^4y e^{ip' \cdot x} e^{iq \cdot y} \Pi_{\mu\nu\alpha}(x, y), \text{ with } \Pi_{\mu\nu\alpha}(x, y) = \langle 0 | T[j_\mu^\psi(x) j_\nu^V(y) j_\alpha^{X^\dagger}(0)] | 0 \rangle, \quad (5)$$

where $p = p' + q$ and the interpolating fields are given by:

$$j_\mu^\psi = \bar{c}_a \gamma_\mu c_a, \quad (6)$$

$$j_\nu^V = \frac{N}{2} (\bar{u}_a \gamma_\nu u_a + (-1)^I \bar{d}_a \gamma_\nu d_a), \quad (7)$$

with $N = I = 1$ for $V = \rho$, $N = 1/3$, $I = 0$ for $V = \omega$ and

$$j_\alpha^X = a j_\alpha^u + b j_\alpha^d, \quad (8)$$

where j_α^q is given in Eq.(2) and (see Eq.(4)).

$$\text{for } X_l \begin{cases} a = \cos \theta \\ b = \sin \theta \end{cases}, \quad \text{for } X_h \begin{cases} a = -\sin \theta \\ b = \cos \theta \end{cases} \quad (9)$$

Using the above definitions in Eq.(5) we arrive at

$$\Pi_{\mu\nu\alpha}(x, y) = \frac{-iN}{2\sqrt{2}} (a \Pi_{\mu\nu\alpha}^u(x, y) + (-1)^I b \Pi_{\mu\nu\alpha}^d(x, y)), \quad (10)$$

with

$$\Pi_{\mu\nu\alpha}^q(x, y) = \epsilon_{abc} \epsilon_{dec} \text{Tr} \left[S_{ea'b}^c(x) \gamma_\mu S_{a'b}^c(x) (\gamma_5 C S_{b'a}^{qT}(y) C \gamma_\nu C S_{db'}^{qT}(-y) C \gamma_\alpha - \gamma_\alpha C S_{b'a}^{qT}(y) C \gamma_\nu C S_{db'}^{qT}(-y) C \gamma_5) \right], \quad (11)$$

where $S_{ab}^q(x - y) = \langle 0 | T[q_a(x) \bar{q}_b(y)] | 0 \rangle$ is the full quark q propagator.

To evaluate the phenomenological side of the sum rule we insert, in Eq.(5), intermediate states for X , J/ψ and V . Using the definitions:

$$\langle 0 | j_\mu^\psi | J/\psi(p') \rangle = m_\psi f_\psi \epsilon_\mu(p'), \quad \langle 0 | j_\nu^V | V(q) \rangle = m_V f_V \epsilon_\nu(q), \quad \langle X_q(p) | j_\alpha^q | 0 \rangle = \lambda_q \epsilon_\alpha^*(p), \quad (12)$$

we obtain the following relation:

$$\Pi_{\mu\nu\alpha}^{q(phen)}(p, p', q) = \frac{\lambda_q m_\psi f_\psi m_V f_V g_{X\psi V}(q^2)}{(p^2 - m_X^2)(p'^2 - m_\psi^2)(q^2 - m_V^2)} \left(-\epsilon^{\alpha\mu\nu\sigma} (p'_\sigma + q_\sigma) - \epsilon^{\alpha\mu\sigma\gamma} \frac{p'_\sigma q_\gamma q_\nu}{m_V^2} - \epsilon^{\alpha\nu\sigma\gamma} \frac{p'_\sigma q_\gamma p'_\mu}{m_\psi^2} \right) + \dots, \quad (13)$$

where the dots stand for the contribution of all possible excited states, and the form factor, $g_{X\psi V}(q^2)$, is defined by the generalization of the on-mass-shell matrix element, $\langle J/\psi V | X \rangle$, for an off-shell V meson:

$$\langle J/\psi(p') V(q) | X(p) \rangle = g_{X\psi V}(q^2) \epsilon^{\sigma\alpha\mu\nu} p_\sigma \epsilon_\alpha(p) \epsilon_\mu^*(p') \epsilon_\nu^*(q), \quad (14)$$

which can be extracted from the effective Lagrangian that describes the coupling between two vector mesons and one axial vector meson [4]:

$$\mathcal{L} = i g_{X\psi V} \epsilon^{\mu\nu\alpha\sigma} (\partial_\mu X_\nu) \Psi_\alpha V_\sigma. \quad (15)$$

From Eq.(13) we see that we have four independent structures in the phenomenological side. For each one of these structures, i , we can write

$$\Pi_i^{q(phen)} \frac{A_i g_{X\psi V}(q^2)}{(q^2 - m_V^2)(p^2 - m_X^2)(p'^2 - m_\psi^2)} + \int_{4m_c^2}^\infty \frac{\rho_i^{cont}(p^2, q^2, u)}{u - p'^2} du. \quad (16)$$

In Eq.(16), $\rho_i^{cont}(p^2, q^2, u)$, gives the continuum contributions, which can be parametrized as $\rho_i^{cont}(p^2, q^2, u) = \frac{b_i(u, q^2)}{s_0 - p^2} \Theta(u - u_0)$ [20, 21, 22], with s_0 and u_0 being the continuum thresholds for X and J/ψ respectively. Taking the limit $p^2 = p'^2 = -P^2$ and performing a single Borel transformation to $P^2 \rightarrow M^2$, we get ($Q^2 = -q^2$):

$$\Pi_i^{q(phen)}(M^2) = \frac{A_i g_{X\psi V}(Q^2)}{(m_V^2 + Q^2)(m_X^2 - m_\psi^2)} \left(e^{-m_\psi^2/M^2} - e^{-m_X^2/M^2} \right) + \frac{B_i}{(m_V^2 + Q^2)} e^{-s_0/M^2} + \int_{u_0}^{\infty} \rho_i^{cc}(u, Q^2) e^{-u/M^2} du, \quad (17)$$

where B_i and $\rho_i^{cc}(u, Q^2)$ stand for the pole-continuum transitions and pure continuum contributions. For simplicity, one assumes that the pure continuum contribution to the spectral density, $\rho_i^{cc}(u, Q^2)$, is given by the result obtained in the OPE side for the structure i . Asymptotic freedom ensures this equivalence for sufficiently large u . Therefore, one uses the Ansatz: $\rho_i^{cc}(u, Q^2) = \rho_i^{OPE}(u, Q^2)$. In Eq.(17), B_i is a parameter which, together with the form factor, $g_{X\psi V}(Q^2)$, has to be determined from the sum rule.

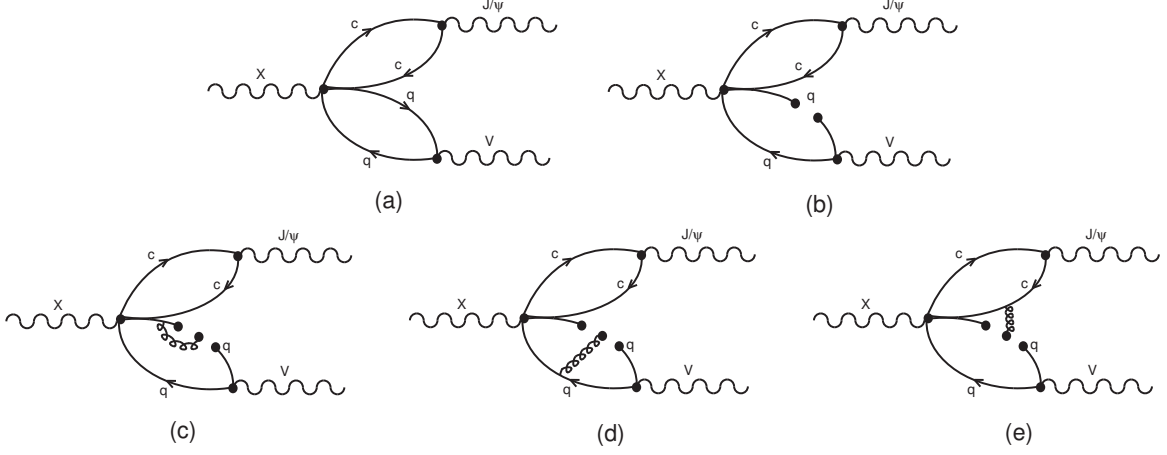


FIG. 1: Diagrams which contribute to the OPE side of the sum rule.

In the OPE side we work at leading order and consider the condensates up to dimension five, as shown in Fig. 1. To keep the charm quark mass finite, we use the momentum-space expression for the charm quark propagator. We calculate the light quark part of the correlation function in the coordinate-space, which is then Fourier transformed to the momentum space in D dimensions. The resulting light-quark part is combined with the charm-quark part before it is dimensionally regularized at $D = 4$. For each structure i , we can write the Borel transform of the correlation function in the OPE side in terms of a dispersion relation:

$$\Pi_i^{q(OPE)}(M^2, Q^2) = \int_{4m_c^2}^{\infty} \rho_i^{q(OPE)}(u, Q^2) e^{-u/M^2} du, \quad (18)$$

where the spectral density, $\rho_i^{q(OPE)}$, is given by the imaginary part of the correlation function. The perturbative term (diagram in Fig. 1(a)) contributes only to the structures $\epsilon^{\alpha\mu\nu\sigma} p'_\sigma$ and $\epsilon^{\alpha\mu\sigma\gamma} p'_\sigma q_\gamma q_\nu$, while the quark condensate and mixed condensate (diagrams (b) to (e) in Fig. 1) contribute to the structures $\epsilon^{\alpha\mu\nu\sigma} q_\sigma$ and $\epsilon^{\alpha\nu\sigma\gamma} p'_\sigma q_\gamma p'_\mu$. Therefore, to get more terms contributing in the OPE side we have two options for the structures: $\epsilon^{\alpha\mu\nu\sigma} q_\sigma$ and $\epsilon^{\alpha\nu\sigma\gamma} p'_\sigma q_\gamma p'_\mu$. In order to test the dependence of the results with the chosen structure, we will work with these two structures.

Transferring the pure continuum contribution to the OPE side we get for the structure $\epsilon^{\alpha\nu\sigma\gamma} p'_\sigma q_\gamma p'_\mu$ (which we call structure 1):

$$\begin{aligned} \Pi_1^{q(OPE)}(M^2, Q^2) &= \frac{i\langle\bar{q}q\rangle}{3\pi^2 Q^2} \left[\left(\frac{m_0^2}{3Q^2} - 1 \right) \int_{4m_c^2}^{u_0} du e^{-u/M^2} \sqrt{1 - 4m_c^2/u} \left(\frac{1}{2} + \frac{m_c^2}{u} \right) + \right. \\ &\quad \left. - \frac{m_0^2}{2^5} \int_0^1 d\alpha \frac{1+3\alpha}{\alpha} e^{\frac{-m_c^2}{\alpha(1-\alpha)M^2}} \right], \end{aligned} \quad (19)$$

and for the structure $\epsilon^{\alpha\mu\nu\sigma} q_\sigma$ (which we call structure 2) we get:

$$\Pi_2^{q(OPE)}(M^2, Q^2) = \frac{i\langle\bar{q}q\rangle}{3\pi^2 Q^2} \left[\left(\frac{m_0^2}{3Q^2} - 1 \right) \int_{4m_c^2}^{u_0} du e^{-u/M^2} u \sqrt{1 - 4m_c^2/u} \left(\frac{1}{2} + \frac{m_c^2}{u} \right) + \right.$$

$$- \frac{m_0^2 m_c^2}{2^5} \int_0^1 d\alpha \frac{1+3\alpha}{\alpha^2(1-\alpha)} e^{\frac{-m_c^2}{\alpha(1-\alpha)M^2}} \Big]. \quad (20)$$

In Eqs. (19) and (20) we have used the relation $\langle \bar{q}g\sigma.Gq \rangle = m_0^2 \langle \bar{q}q \rangle$.

Making use of Eqs. (9) and (10), and working at the SU(2) limit, *i.e.*, considering the quarks u and d degenerate, we arrive at three sum rules for each structure, that can be written in the general expression:

$$C_i^{XV}(Q^2) \left(e^{-m_\psi^2/M^2} - e^{-m_X^2/M^2} \right) + B_i e^{-s_0/M^2} = -i \frac{Q^2 + m_V^2}{2\sqrt{2}} \Pi_i^{q(OPE)}(M^2, Q^2), \quad (21)$$

where

$$C_1^{XV}(Q^2) = \frac{f_\psi}{m_\psi} \frac{\lambda_q}{m_X^2 - m_\psi^2} A_{XV}(Q^2), \text{ and } C_2^{XV}(Q^2) = f_\psi m_\psi \frac{\lambda_q}{m_X^2 - m_\psi^2} A_{XV}(Q^2), \quad (22)$$

and

$$\begin{aligned} A_{X_l\rho}(Q^2) &= m_\rho f_\rho \frac{\cos\theta + \sin\theta}{\cos\theta - \sin\theta} g_{X_l\psi\rho}(Q^2), \\ A_{X_h\rho}(Q^2) &= -m_\rho f_\rho \frac{\cos\theta - \sin\theta}{\cos\theta + \sin\theta} g_{X_h\psi\rho}(Q^2), \\ A_{X_l\omega}(Q^2) &= A_{X_h\omega}(Q^2) = 3m_\omega f_\omega g_{X_l\psi\omega}(Q^2). \end{aligned} \quad (23)$$

Since from Eq.(21) we see that the OPE side of the sum rule determines only one value for C^{XV} for each structure (for a fixed value of Q^2), we arrive at the following relations between the form factors:

$$\begin{aligned} \frac{g_{X_l\psi\omega}(Q^2)}{g_{X_l\psi\rho}(Q^2)} &= \frac{m_\rho f_\rho}{3m_\omega f_\omega} \frac{\cos\theta + \sin\theta}{\cos\theta - \sin\theta}, \\ \frac{g_{X_h\psi\omega}(Q^2)}{g_{X_h\psi\rho}(Q^2)} &= -\frac{m_\rho f_\rho}{3m_\omega f_\omega} \frac{\cos\theta - \sin\theta}{\cos\theta + \sin\theta}. \end{aligned} \quad (24)$$

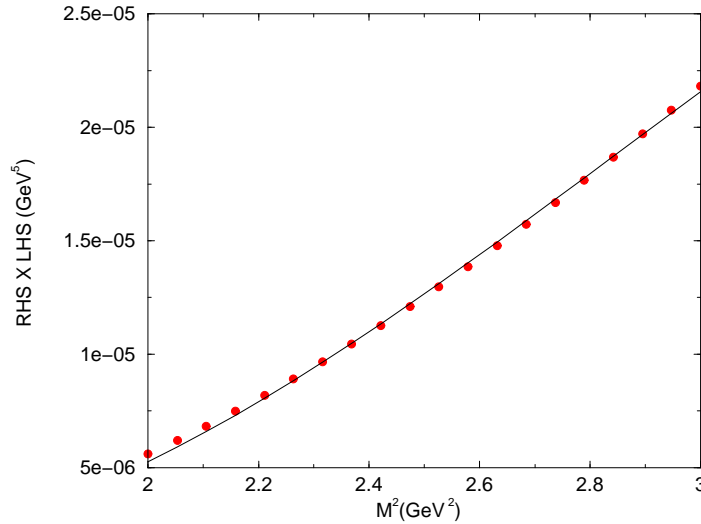


FIG. 2: Dots: the RHS of Eq.(21), as a function of the Borel mass for $Q^2 = 3 \text{ GeV}^2$. The solid line gives the fit of the QCDSR results through the LHS of Eq.(21) for $\Delta s_0 = 0.5 \text{ GeV}$.

In the numerical analysis of the sum rules, the values used for the quark masses and condensates are: $m_c = 1.2 \text{ GeV}$, $\langle \bar{q}q \rangle = -(0.23)^3 \text{ GeV}^3$, $m_0^2 = 0.8 \text{ GeV}^2$. For the meson parameters we use their experimental values [23]: $m_\rho = 0.776 \text{ GeV}$, $m_\omega = 0.782 \text{ GeV}$, $m_\psi = 3.1 \text{ GeV}$, $m_X = 3.872 \text{ GeV}$, $f_\rho = 0.157 \text{ GeV}$, $f_\omega = 0.046 \text{ GeV}$ and $f_\psi = 0.405 \text{ GeV}$. We evaluate our sum rules in the range $2.0 \leq M^2 \leq 3.0$, which is the range where the two-point function for $X(3872)$ shows good OPE convergence and where the pole contribution is bigger than the continuum

contribution [19]. We also use three different values for $s_0 = (3.872 + \Delta s_0)^2 \text{ GeV}^2$: $\Delta s_0 = 0.4 \text{ GeV}$, $\Delta s_0 = 0.5 \text{ GeV}$ and $\Delta s_0 = 0.6 \text{ GeV}$. For u_0 we use $u_0 = (m_\psi + 0.5)^2 \text{ GeV}^2$. The meson-current coupling, λ_q , defined in Eq.(12), can be determined from the two-point sum rule [19]. In Table I we give the results obtained from ref.[19] for three different values of s_0 .

Table I: Numerical results for the meson-current coupling

| $\lambda_q \text{ (GeV}^5\text{)}$ | $\Delta s_0 \text{ (GeV)}$ |
|------------------------------------|----------------------------|
| $(1.85 \pm 0.01) \times 10^{-2}$ | 0.4 |
| $(1.94 \pm 0.03) \times 10^{-2}$ | 0.5 |
| $(2.02 \pm 0.06) \times 10^{-2}$ | 0.6 |

We start with the structure 1. In Fig. 2 we show, through the circles, the right-hand side (RHS) of Eq.(21) for $Q^2 = 3 \text{ GeV}^2$, as a function of the Borel mass.

To determine $g_{X\psi V}(Q^2)$ we fit the QCDSR results with the analytical expression in the left-hand side (LHS) of Eq.(21), and we get (using $\Delta s_0 = 0.5 \text{ GeV}$): $C_1^{XV}(Q^2 = 3 \text{ GeV}^2) = 7.01 \times 10^{-4} \text{ GeV}^5$ and $B_1 = -1.28 \times 10^{-3} \text{ GeV}^5$. Using the definition of $C_1^{XV}(Q^2)$ in Eq.(22) we get $A_{XV}(Q^2 = 3 \text{ GeV}^2) = 1.49 \text{ GeV}^2$. Allowing Q^2 to vary in the interval $2.5 \leq Q^2 \leq 4.5 \text{ GeV}^2$, we show, in Fig. 3, through the circles, the momentum dependence of $A_{XV}(Q^2)$.

From Eq.(23), we see that all form factors are related with the function $A_{XV}(Q^2)$. Since the coupling constant is defined as the value of the form factor at the meson pole: $Q^2 = -m_V^2$, to determine the coupling constant we have to extrapolate the QCDSR results to a Q^2 region where the sum rules are no longer valid (since the QCDSR results are valid in the deep Euclidian region). To do that we parametrize the QCDSR results through a analytical form. In Fig. 3 we also show that the Q^2 dependence of $A_{XV}(Q^2)$ can be well reproduced by the monopole parametrization (solid line):

$$A_{XV}(Q^2) = \frac{66.8}{Q^2 + 41.8}, \quad (25)$$

from where we can extract the value of $A_{XV}(Q^2)$ at the meson pole: $A_{XV}(Q^2 = -m_V^2) = 1.62 \text{ GeV}^2$.

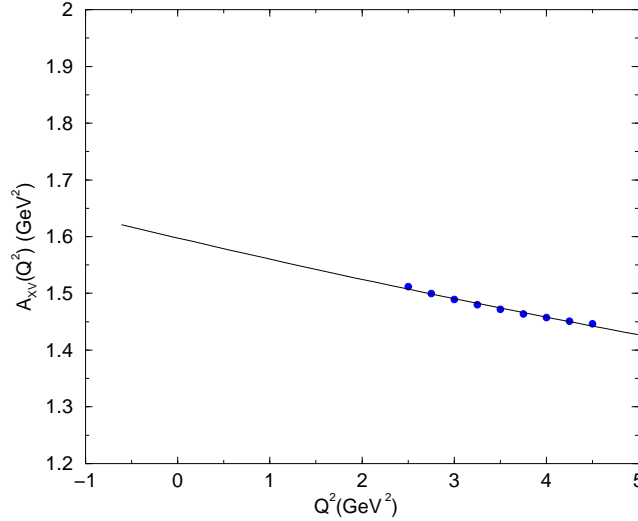


FIG. 3: Momentum dependence of A_{XV} for $\Delta s_0 = 0.5 \text{ GeV}$. The solid line gives the parametrization of the QCDSR results (circles) through Eq. (25).

Doing the same kind of analysis for the other values of the continuum threshold we show, in Table II, the monopole parametrizations of the QCDSR results, as well as their values at the off-shell meson pole.

Table II: Monopole parametrization of the QCDSR results for the structure 1, for different values of Δs_0

| $\Delta s_0 \text{ (GeV)}$ | $A_{XV}(Q^2) \text{ (GeV}^2\text{)}$ | $A_{XV}(Q^2 = -m_V^2) \text{ (GeV}^2\text{)}$ |
|----------------------------|--------------------------------------|---|
| 0.4 | $\frac{70.2}{Q^2 + 41.6}$ | 1.71 |
| 0.5 | $\frac{66.8}{Q^2 + 41.8}$ | 1.62 |
| 0.6 | $\frac{63.8}{Q^2 + 41.7}$ | 1.55 |

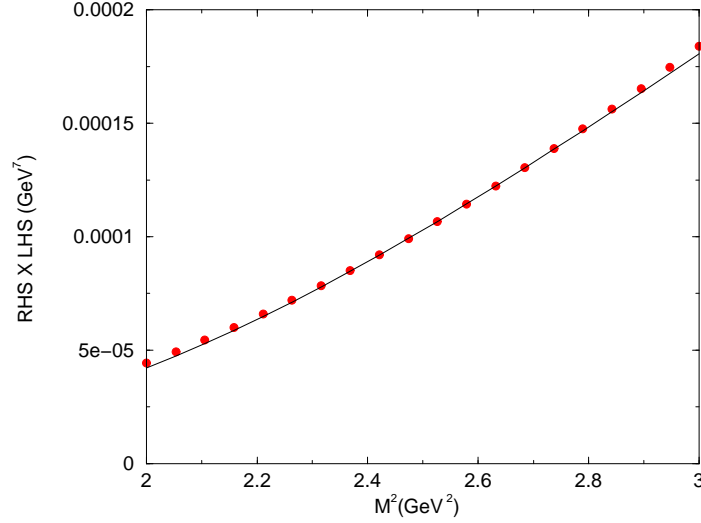


FIG. 4: Dots: the RHS of Eq.(21), for the structure 2, as a function of the Borel mass for $Q^2 = 3 \text{ GeV}^2$. The solid line gives the fit of the QCDSR results through the LHS of Eq.(21) for $\Delta s_0 = 0.4 \text{ GeV}$.

In the case of the structure 2, the RHS of Eq.(21) can also be very well parametrized with the analytical expression in the LHS of Eq.(21), as can be seen in Fig. 4. We get (using $\Delta s_0 = 0.4 \text{ GeV}$): $C_2^{XV}(Q^2 = 3 \text{ GeV}^2) = 5.56 \times 10^{-3} \text{ GeV}^7$ and $B_2 = -3.46 \times 10^{-3} \text{ GeV}^7$. Using the definition of $C_2^{XV}(Q^2)$ in Eq.(22) we get $A_{XV}(Q^2 = 3 \text{ GeV}^2) = 1.29 \text{ GeV}^2$. The Q^2 behaviour of $A_{XV}(Q^2)$ can also be well represented by a monopole form in the case of structure 2, with a precision similar to the one shown in Fig. 3. In Table III we give the monopole parametrizations of the QCDSR results for the structure 2, as well as their values at the off-shell meson pole.

Table III: Monopole parametrization of the QCDSR results for the structure 2, for different values of Δs_0

| $\Delta s_0 \text{ (GeV)}$ | $A_{XV}(Q^2) \text{ (GeV}^2\text{)}$ | $A_{XV}(Q^2 = -m_V^2) \text{ (GeV}^2\text{)}$ |
|----------------------------|--------------------------------------|---|
| 0.4 | $\frac{59.0}{Q^2 + 42.6}$ | 1.45 |
| 0.5 | $\frac{56.0}{Q^2 + 42.8}$ | 1.34 |
| 0.6 | $\frac{54.2}{Q^2 + 42.9}$ | 1.28 |

Comparing the results in Tables II and III we see that, although the results from the structure 2 are somewhat smaller than the results from the structure 1, they are still compatible with each other. We will use these differences to estimate the uncertainties in our results.

From Eq. (23) we see that, in the case of the meson ω , there is no mixing angle dependence in the relation between A_{XV} and $g_{X\psi\omega}$. Therefore we can use the results in Tables II and III to directly estimate the $XJ/\psi\omega$ coupling constant. We get

$$g_{X\psi\omega} = 13.8 \pm 2.0, \quad (26)$$

which is much bigger than the guess made in ref.[4]: $g_{X\psi V} = 0.475$.

Having the coupling constant and the relations in Eqs. (23) and (24), we can estimate the decay widths of the processes $X \rightarrow J/\psi \pi^+ \pi^- \pi^0$ and $X \rightarrow J/\psi \pi^+ \pi^-$ by supposing that the 2π and 3π decays are dominated by the ρ and ω vector mesons respectively. In the narrow width approximation we have:

$$\frac{d\Gamma}{ds}(X \rightarrow J/\psi(n\pi)) = \frac{1}{8\pi m_X^2} |\mathcal{M}|^2 \frac{m_X^2 - m_\psi^2 + s}{2m_X^2} \frac{\Gamma_V m_V}{\pi} \frac{p(s)}{(s - m_V^2)^2 + (m_V \Gamma_V)^2} B_{V \rightarrow n\pi}, \quad (27)$$

with $n = 2, 3$ for $V = \rho, \omega$. In Eq.(27), s is the invariant mass-squared of the pions, Γ_V and $B_{V \rightarrow n\pi}$ are, respectively, the total decay width and the branching ratio of the $V \rightarrow n\pi$ decay. The decay momentum $p(s)$ is given by

$$p(s) = \frac{\sqrt{\lambda(m_X^2, m_\psi^2, s)}}{2m_X}, \quad (28)$$

with $\lambda(a, b, c) = a^2 + b^2 + c^2 - 2ab - 2ac - 2bc$.

The invariant amplitude squared can be obtained from the matrix element in Eq.(14). We get:

$$|\mathcal{M}|^2 = \frac{g_{X\psi V}^2}{3} \left(4m_X^2 - \frac{m_\psi^2 + s}{2} + \frac{(m_X^2 - m_\psi^2)^2}{2s} + \frac{(m_X^2 - s)^2}{2m_\psi^2} \right), \quad (29)$$

where we have replaced the form factor, $g_{X\psi V}(s)$ by the coupling constant $g_{X\psi V}$, since from Tables II and III we can see that the form factor is very flat over the region, $(n\ m_\pi)^2 \leq s \leq (m_X - m_\psi)^2$, over which Eq.(27) will be integrated. Using the relations between the coupling constants from Eq.(24) we get the following relations between the decay widths:

$$\begin{aligned} \left(\frac{\Gamma(X_l \rightarrow J/\psi\ 3\pi)}{\Gamma(X_l \rightarrow J/\psi\ 2\pi)} \right) &= \frac{m_\rho^2 f_\rho^2}{9m_\omega^2 f_\omega^2} \left(\frac{\cos\theta + \sin\theta}{\cos\theta - \sin\theta} \right)^2 \frac{I_\omega}{I_\rho}, \\ \left(\frac{\Gamma(X_h \rightarrow J/\psi\ 3\pi)}{\Gamma(X_h \rightarrow J/\psi\ 2\pi)} \right) &= \frac{m_\rho^2 f_\rho^2}{9m_\omega^2 f_\omega^2} \left(\frac{\cos\theta - \sin\theta}{\cos\theta + \sin\theta} \right)^2 \frac{I_\omega}{I_\rho}, \end{aligned} \quad (30)$$

where we have defined

$$\begin{aligned} I_V &= \frac{\Gamma_V m_V}{\pi} \int_{(n\ m_\pi)^2}^{(m_X - m_\psi)^2} ds \left[\left(4m_X^2 - \frac{m_\psi^2 + s}{2} + \frac{(m_X^2 - m_\psi^2)^2}{2s} + \frac{(m_X^2 - s)^2}{2m_\psi^2} \right) \times \right. \\ &\quad \times \left. \frac{m_X^2 - m_\psi^2 + s}{2m_X^2} \frac{p(s)}{(s - m_V^2)^2 + (m_V \Gamma_V)^2} \right] B_{V \rightarrow n\pi}. \end{aligned} \quad (31)$$

Since the relations in Eq.(30) do not depend on the value of the coupling constant we get

$$\left(\frac{\Gamma(X_{l,h} \rightarrow J/\psi\ 3\pi)}{\Gamma(X_{l,h} \rightarrow J/\psi\ 2\pi)} \right) = 0.152 \left(\frac{\cos\theta \pm \sin\theta}{\cos\theta \mp \sin\theta} \right)^2. \quad (32)$$

Therefore, using the central experimental data given in Eq.(1) we obtain for the mixing angle

$$\theta \simeq \pm 23.5^\circ \quad (33)$$

for X_l or X_h respectively, which is in agreement with the result obtained in [4]: $\theta \simeq \pm 20^\circ$.

Since, with the determination of the mixing angle in Eq.(33) by imposing the ratio in Eq.(1), we obtain the same width for any of the four decays in Eq.(30), we can use the value of the coupling constant determined in Eq.(26) to evaluate the partial decay width. We get

$$\Gamma(X \rightarrow J/\psi\ (n\pi)) = (50 \pm 15) \text{ MeV}, \quad (34)$$

which is much bigger than the experimental total width: $\Gamma(X(3872)) < 2.3 \text{ MeV}$.

As a matter of fact, a large partial decay width was expected in this case. The initial state already contains all the four quarks needed for the decay, and there is no violating rules prohibiting the decay. Therefore, the decay is allowed as in the case of the light scalars σ and κ studied in [17], which widths are of the order of 400 MeV. However, even when there is no violating rules prohibiting the decay, the decay can be prevented due to a non-trivial color structure in the initial state. In ref.[22], an alternative technique was developed to obtain the form factor and coupling constant for multiquark particles. By multiquark we mean that the initial state contains the same number of valence quarks as the number of valence quarks in the final states. In this case, as can be seen in Fig. 1, the generic decay diagram in terms of quarks has two “petals”, one associated with the J/ψ and the other with the other vector meson V . Among the diagrams in Fig. 1 there are two distinct subsets. In the first (diagrams from (a) to (d)) there is no gluon line connecting the petals and, therefore, no color exchange between the two final mesons in the decay. A diagram of this type was called color-disconnected (CD) diagrams in ref. [22]. If there is no color exchange, the final state containing two color singlets was already present in the initial state. In this case the tetraquark had a component similar to a $J/\psi - V$ molecule. The other subset of diagrams is represented by diagram in Fig. 1(e), where there is a color exchange between the petals. This type of diagram represents the case where the X is a genuine four-quark state with a complicated color structure. These diagrams are called color-connected (CC). In our approach we have considered all kinds of diagrams. However, if we consider only the CC diagrams, which means considering only the diagram (e) in Fig. 1, we get $g_{X\psi\omega}^{(CC)} = 1.6 \pm 0.3$, and therefore

$$\Gamma_{CC}(X \rightarrow J/\psi\ (n\pi)) = (0.7 \pm 0.2) \text{ MeV}. \quad (35)$$

This procedure may appear somewhat unjustified. However, we do believe that there should be a particular choice of the interpolating field, which represents a genuine four-quark state, for which CD diagrams vanish. From our calculation we find out that the interpolating field in Eq.(2) has a component similar to a $J/\psi - V$ molecule.

To summarize: we have presented a QCD sum rule study of the three-point functions of the hadronic decays of $X(3872)$ meson, considered as a diquark antidiquark four quark state. Supposing that the physical state is a mixture between the isospin eigenstates, we find that the QCD sum rules result for the mixing angle is compatible with the result found in [4]. However, we get a partial decay width much bigger than the experimental total decay width. Therefore, we conclude that our particular choice of the interpolating field has a $J/\psi V$ molecule component, and is not the most appropriate candidate to explain the very small width of the meson $X(3872)$. Further studies, using different interpolating fields, are necessary for a better understanding of the structure of the meson $X(3872)$.

-
- [1] BABAR Coll., B. Auber *et al.*, Phys. Rev. Lett. **90**, 242001 (2003); Phys. Rev. **D69**, 031101 (2004); CLEO Coll., D. Besson *et al.*, Phys. Rev. **D68**, 032002 (2003); BELLE Coll., P. Krokovny *et al.*, Phys. Rev. Lett. **91**, 262002 (2003).
 - [2] S.-L. Choi *et al.* [Belle Collaboration], Phys. Rev. Lett. **91**, 262001 (2003); V. M. Abazov *et al.* [D0 Collaboration], Phys. Rev. Lett. **93**, 162002 (2004); D. Acosta *et al.* [CDF II Collaboration], Phys. Rev. Lett. **93**, 072001 (04); B. Aubert *et al.* [BABAR Collaboration], Phys. Rev. D **71**, 071103 (2005).
 - [3] K. Abe *et al.* [Belle Collaboration], hep-ex/0505037, hep-ex/0505038.
 - [4] L. Maiani, F. Piccinini, A.D. Polosa, V. Riquer, Phys. Rev. **D71**, 014028 (2005).
 - [5] H. Hogaasen, J.-M. Richard, P. Sorba, Phys. Rev. **D73**, 054013 (2006).
 - [6] D. Bugg, Phys. Lett. **B598**, 8 (2004).
 - [7] B.-A. Li, Phys. Lett. **B605**, 306 (2005).
 - [8] K. K. Seth, Phys. Lett. B **612**, 1 (2005).
 - [9] N. Tornqvist, hep-ph/0308277.
 - [10] F.E. Close and P. Page, Phys. Lett. **B578**, 119 (2004).
 - [11] C.Y. Wong, Phys. Rev. **C69**, 055202 (2004).
 - [12] S. Pakvasa and M. Suzuki, Phys. Lett. **B579**, 67 (2004).
 - [13] E. S. Swanson, Phys. Lett. B **588**, 189 (2004); Phys. Lett. B **598**, 197 (2004); hep-ph/0601110.
 - [14] M.A. Shifman, A.I. and Vainshtein and V.I. Zakharov, Nucl. Phys. **B147**, 385 (1979).
 - [15] L.J. Reinders, H. Rubinstein and S. Yazaky, Phys. Rep. **127**, 1 (1985).
 - [16] For a review and references to original works, see e.g., S. Narison, *QCD as a theory of hadrons, Cambridge Monogr. Part. Phys. Nucl. Phys. Cosmol.* **17** (2002) 1-778 [hep-h/0205006]; *QCD spectral sum rules*, *World Sci. Lect. Notes Phys.* **26** (1989) 1-527; *Acta Phys. Pol.* **26** (1995) 687; *Riv. Nuov. Cim.* **10N2** (1987) 1; *Phys. Rep.* **84** (1982).
 - [17] T.V. Brito *et al.*, Phys. Lett. **B608**, 69 (2005).
 - [18] M.E. Bracco *et al.*, Phys. Lett. **B624**, 217 (2005).
 - [19] R. Matheus, S. Narison, M. Nielsen and J.-M. Richard, to appear.
 - [20] M. Nielsen, Phys. Lett. **B634**, 35 (2006).
 - [21] B. L. Ioffe and A.V. Smilga, Nucl. Phys. **B232**, 109 (1984).
 - [22] M. Eidemüller *et al.*, Phys. Rev. **D72**, 034003 (2005).
 - [23] S. Eidelman *et al.*, Phys. Lett. **B592**, 1 (2004).